Pinning Mechanism Studies on the Nb/Ag Superconducting Multilayer

1993 Jpn. J. Appl. Phys. 32 1952

(http://iopscience.iop.org/1347-4065/32/5R/1952)

Jpn. J. Appl. Phys. Vol. 32 (1993) pp. 1952–1955
Part 1, No. 5A, May 1993

Pinning Mechanism Studies on the Nb/Ag Superconducting Multilayer

Yoshihisa OBI, Manabu IKEBE[1], Hiroyuki FUJISHIRO[1] and Hiroyasu FUJIMORI
Institute for Materials Research, Tohoku University, Sendai 980
[1]*Department of Materials Science, Faculty of Engineering, Iwate University, Morioka 020*

(Received January 14, 1993; accepted for publication March 13, 1993)

The critical currents of the Nb/Ag multilayer, a proximity-effect-coupled artificial layered superconductor, have been measured. The behavior of the flux pinning force is compared with that of the Nb/Al_2O_3 multilayer, a previously studied Josephson-coupled layered superconductor. Several qualitative and quantitative differences in the pinning characteristics of the two systems are pointed out.

KEYWORDS: superconductor, upper critical field, critical current, pinning force, superlattice, multilayer

1. Introduction

Superconducting properties of a material are greatly influenced by multilayering. For layered structures, it is well known that the critical field parallel to the plane can be markedly enhanced.[1-5] It is also expected that the layered structure may play a role as a pinning center and contribute to the enhancement of the critical current J_c. Therefore the artificial multilayered superconductor seems to be an interesting object of investigation from both fundamental and applicational physical points of view.

The superconducting multilayer may be divided into two main categories according to the type of interlayer coupling. One is superconductor/metal multilayers in which the interlayer coupling is due to the proximity effect. The other is the superconductor/insulator multilayers in which the interlayer coupling is due to Josephson tunneling. Theoretical studies on superconducting properties appropriate for each type of multilayer have already been reported by several authors.[6-11] We have applied an rf dual-sputtering technique to the study of superconducting properties of Nb-based multilayered systems.[12-15] As a model system of Josephson coupled multilayers, we fabricated Nb/Al_2O_3 multilayers and investigated the pinning characteristics as reported in previous papers.[16,17] There we pointed out that the cross-plane pinning force density $F_{p\perp}$ shows peculiar behavior which depends on the superconductive dimensionality; the maximum point of the reduced pinning curve $F_{p\perp}/F_{p\perp mix}$ vs h $(=H/H_{c2})$ shifted from a rather low h value in three-dimensional (3D) multilayers to a very high h value in two-dimensional (2D) ones. In this study we examine if the above-mentioned anomalous shift accompanied with the change of the superconductivity is observable also in a proximity-effect-coupled system, the Nb/Ag multilayer. The possibility of using the Nb/Ag for practical application as a superconducting material is also discussed.

2. Experimental

Critical current measurements were performed on the Nb/Ag specimens with the structural modulation wavelength λ=44 Å, 159 Å, 465 Å and 736 Å. Nb and Ag do not form solid solution, so we selected Nb/Ag system so as to minimize the interdiffusion through the boundary. By use of a low-angle X-ray diffractometer, satellite peaks were observed for all samples, which confirmed the existence of the modulated layer structure. The λ values were determined from the position of the satellite peaks. The layer thicknesses of Nb (dNb) and Ag (dAg) sublayers were designed to be equal, so that $\lambda=2d\text{Nb}=2d\text{Ag}$. The superconductive dimensionality was determined from the behavior of the parallel critical field ($H_{c2/\!/}$) shown in Fig. 1(a). In the

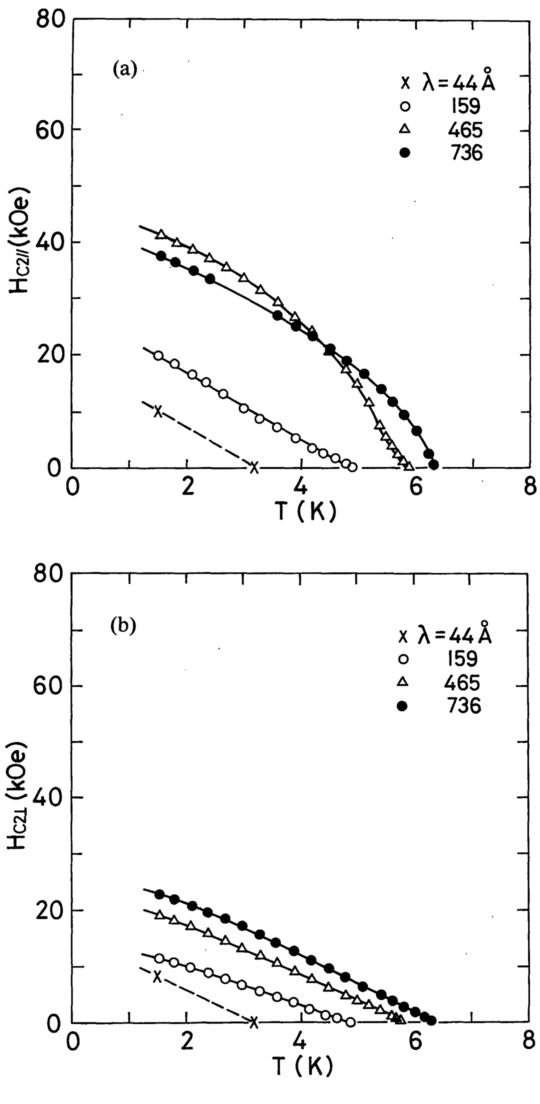

Fig. 1. Upper critical field as a function of temperature of Nb/Ag multilayers with λ=44, 159, 465 and 736 Å. (a) Parallel critical field ($H_{c2/\!/}$), (b) perpendicular critical field ($H_{c2\perp}$).

Table I. Several Material parameters.

λ (Å)	T_c (K)	$-(dH_{c2\perp}/dT)_{T-T_c}$ (kOe/K)	$H_{c2/\!/}$ at 1.5 K (kOe)	$H_{c2\perp}$ at 1.5 K (kOe)	$H_{c2/\!/}/H_{c2\perp}$	$F_{p\perp max}$ at 1.5 K (10^8 dyn/cm^3)	$F_{p/\!/max}$ at 1.5 K (10^8 dyn/cm^3)	$F_{p\perp max}/F_{p/\!/max}$	$F_{p/\!/max}/H_{c2\perp}$ (10^{10} dyn/cm^3 kOe)	*PEF*
44	3.17	(4.87)	10.43	9.01	1.16	0.014	0.070	2.00	0.78	1.72
159	5.00	3.47	20.38	12.01	1.70	0.500	0.290	1.72	2.41	1.01
465	6.17	4.25	41.52	19.04	2.18	1.18	0.440	2.68	2.31	1.23
736	6.47	4.92	37.59	22.79	1.65	2.90	0.735	3.95	3.22	2.39

case that $H_{c2/\!/}$ is proportional to $(1-T/T_c)^1$ near the transition temperature T_c, the superconductivity is 3D and in the case that $H_{c2/\!/}$ is proportional to $(1-T/T_c)^{1/2}$ near T_c, the superconductivity is 2D. In the multilayered system the superconductivity is expected to be 3D for small values of λ and 2D for large values of λ, with the quasi-2D behavior being usually observable between the 3D and 2D regions.[1,2,18] In Fig. 1(a), the 3D superconductivity is confirmed for $\lambda=44$ Å and 159 Å, and quasi 2D is confirmed for 465 Å and 2D is confirmed for 736 Å. The perpendicular critical field ($H_{c2\perp}$) is shown in Fig. 1(b) for comparison. Experimental details are the same as those described in the previous paper.[16] Several superconducting material parameters are summarized in Table I.

3. Results and Discussion

Figures 2(a) and 2(b) show cross-plane ($F_{p\perp}$) and in-plane ($F_{p/\!/}$) pinning force density at 1.5 K as a function of the applied field $H_{/\!/}$ and $H_\perp$, respectively. Here $H_{/\!/}$ and $H_\perp$ respectively denote the applied field parallel and perpendicular to the multilayer plane. $F_{p\perp}$ and $F_{p/\!/}$ are defined by

$$F_{p\perp}=(1/c)J_{c/\!/}\times H_{/\!/} \quad (1)$$

$$F_{p/\!/}=(1/c)J_{c\perp}\times H_\perp, \quad (2)$$

$J_{c/\!/}$ and $J_{c\perp}$ being the critical current density for $H_{/\!/}$ and $H_\perp$, respectively. Both $F_{p\perp}$ and $F_{p/\!/}$ increase with the increase of λ in the measured region of $\lambda\leqq 736$ Å. $F_{p\perp}$ is always larger than $F_{p/\!/}$, which seems to be a general characteristic of the multilayered structure. In order to obtain detailed pictures of the anisotropy of the pinning force density and its correlation with the upper critical field anisotropy, we plot $H_{c2/\!/}/H_{c2\perp}$, $F_{p\perp max}/F_{p/\!/max}$ and $(F_{p\perp max}/F_{p/\!/max})/(H_{c2/\!/}/H_{c2\perp})$ as a function of λ in Fig. 3. We refer to the last quantity, $(F_{p\perp max}/F_{p/\!/max})/(H_{c2/\!/}/H_{c2\perp})$, as the pinning enhancement factor (*PEF*) as in the previous paper.[17] Because $F_{p/\!/}$ and $H_{c2\perp}$ reflect inplane superconducting properties not directly connected with the multilayered structure, *PEF* represents the ratio of the enhancement of the pinning force to that of the upper critical field caused by the multilayering. Thus in the case of *PEF*$=1$, one may consider that the enhancement of $F_{p\perp}$ and $F_{p/\!/}$ is of approximately equal strength. In Fig. 3 we see that the value of $F_{p\perp}/F_{p/\!/}$ is large in the 2D region, while $H_{c2/\!/}/H_{c2\perp}$ reaches its maximum in the quasi-2D region. The strong enhancement of $F_{p\perp}$ only in the 2D region can also be confirmed from the *PEF* vs λ curves; the *PEF* value is very large only for $\lambda=736$ Å. This result indicates that in the proximity-effect-coupled Nb/Ag system, the Ag sublayer thickness of dAg$\geqq$300 Å is necessary for the multilayered structure to produce fully effective pinning center. In marked contrast, previous studies[16,17] showed that the Al_2O_3 sublayer thickness dAl_2O_3 of ~20 Å is sufficient for the full enhancement of $F_{p\perp}$ in the Josephson-cou-

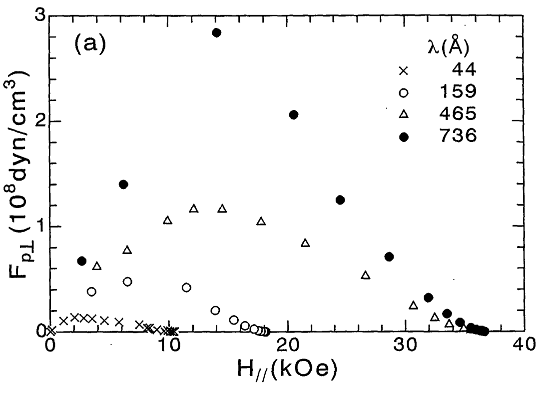

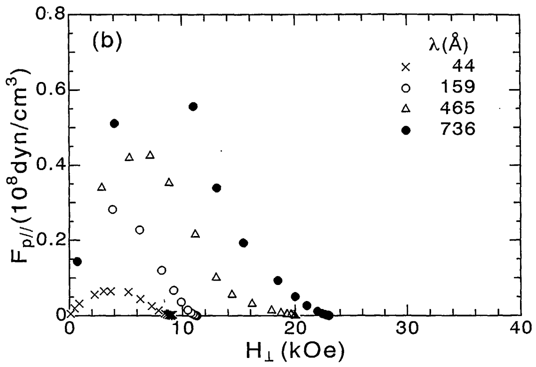

Fig. 2. Pinning force density as a function of applied field at 1.5 K. (a) Cross-plane pinning force ($F_{p\perp}$), (b) in-plane pinning force ($F_{p/\!/}$).

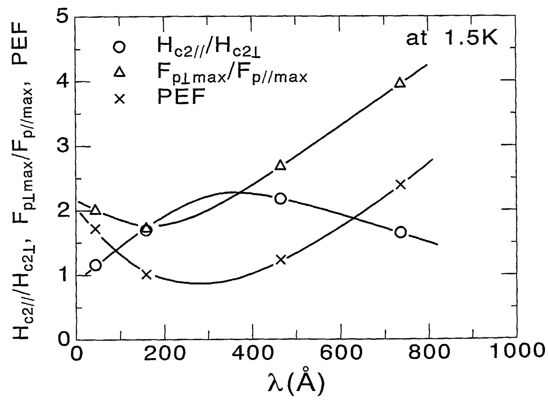

Fig. 3. $H_{c2/\!/}/H_{c2\perp}$, $F_{p\perp max}/F_{p/\!/max}$ and *PEF* $[=(F_{p\perp max}/F_{p/\!/max})/(H_{c2/\!/}/H_{c2\perp})]$ as a function of λ at 1.5 K.

pled Nb/Al_2O_3 system. This quantitative difference is very significant and the insulating Al_2O_3 sublayer is by far the more efficient pinning center in Nb-based multilayered systems. In this respect, the proximity-effect-coupled multilayers seem to have some drawbacks in application as superconducting materials.

The pinning force densities $F_{p\perp max}$ and $F_{p//max}$ of Nb/Ag with $\lambda=44$ Å are very small, although the anisotropy ratio $F_{p\perp max}/F_{p//max}$ is rather large for a 3D multilayer. In order to elucidate the origin of the small F_p, $F_{p//max}/H_{c2\perp}$ values are calculated and compared (see Table I). We notice that $F_{p//max}/H_{c2\perp}$ of the Nb/Ag ($\lambda=44$ Å) sample takes an anomalously small value in comparison with other specimens with larger values of λ. This fact indicates that with this thin dNb, the proximity effect may degrade the current-carrying capacity by, for example, narrowing the effective current path through the superconducting Nb sublayer. On the other hand, even this small structural modulation corresponding to $\lambda=44$ Å works as a somewhat effective pinning center along the direction perpendicular to the layer, thus enhancing the anisotropy $F_{p\perp max}/F_{p//max}$.

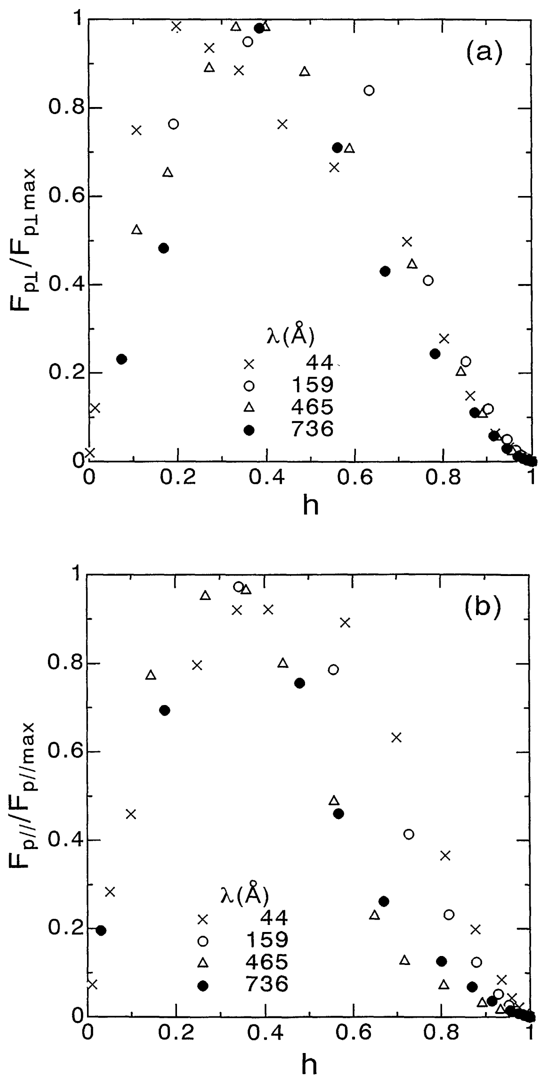

Fig. 4. Reduced pinning force (a) $F_{p\perp}/F_{p\perp max}$ and (b) $F_{p//}/F_{p//max}$ vs reduced field h at 1.5 K.

In Figs. 4(a) and 4(b) the reduced pinning forces $F_{p\perp}/F_{p\perp max}$ and $F_{p//}/F_{p//max}$ are plotted against the reduced field h $(=H/H_{c2})$. For $F_{p\perp}/F_{p\perp max}$ vs h curves (which we refer to as the pinning curves) of the Nb/Al_2O_3 system,[16] we found a clear difference which evidently correlated with the superconductive dimensionality. The peak position of the pinning curves of the Nb/Al_2O_3 multilayers shifted to higher h values, near $h\sim0.8$, from lower h values near $h\sim0.4$, as the superconductive dimensionality changed from 3D to 2D. In Fig. 4(a), the pinning curve of the 2D Nb/Ag multilayer ($\lambda=736$ Å) reaches a maximum at about $h\sim0.35$ and the curve rather coincides with those of the quasi-2D ($\lambda=465$ Å) and the 3D ($\lambda=159$ Å) multilayer. This result indicates that there is a qualitative difference between the cross-plane pinning mechanisms of the Nb/Ag and the Nb/Al_2O_3 systems in the 2D region. Among the Nb/Ag multilayers studied, $F_{p\perp}$ of the 3D specimen with the smallest value of λ ($\lambda=44$ Å) shows a peak position at a very low field (near $h\sim0.20$) distinct from the other Nb/Ag multilayers. This anomalous pinning curve at $\lambda=44$ Å may be related to the anomalously small pinning force densities and to the anomalously large of $F_{p\perp max}/F_{p//max}$ value for this specimen.

4. Summary

(1) The difference in the cross-plane pinning characteristics associated with the change of the superconductive dimensionality is not observable for the Nb/Ag multilayers, which makes a marked contrast to the Nb/Al_2O_3 system. The different superconductive interlayer couplings of the two systems, i.e., the proximity effect and Josephson tunneling, may be responsible for the qualitative difference in the cross-plane pinning mechanisms.

(2) In the measured range of the structural modulation wavelength $\lambda\leqq736$ Å, the pinning force densities of the Nb/Ag system increase with the increase of λ. In particular, the enhancement of the cross-plane pinning force density $F_{p\perp}$ becomes conspicuous when the superconductive dimensionality changes from quasi-2D to 2D. This indicates that the Ag sublayer thickness as large as $d\mathrm{Ag}\geqq300$ Å is necessary to introduce fully effective pinning centers in the Nb/Ag multilayers.

(3) Considering the fact that $d\mathrm{Al_2O_3}\sim20$ Å is sufficient to obtain the maximum pinning force in the Nb/Al_2O_3 system, the metallic Ag sublayer seems to be less efficient than the insulating Al_2O_3 sublayer to introduce powerful pinning centers necessary for application in Nb-based multilayers.

Acknowledgments

This work was partially supported by the Grant-in-Aid for Special Project Research from the Ministry of Education, Science and Culture.

1) S. T. Ruggiero, T. W. Barbee, Jr. and M. R. Beasley: Phys. Rev. B **26** (1982) 4894.
2) I. Banerjee and I. K. Schuller: J. Low Temp. Phys. **54** (1984) 501.

3) C. S. L. Chun, G. G. Zheng, J. L. Vincent and I. K. Schuller: Phys. Rev. B **29** (1984) 4915.
4) J. L. Cohn, J. J. Lin, F. J. Lamelas, H. He, R. Clarke and C. Uher: Phys. Rev. B **38** (1988) 2326.
5) D. Neerinck, K. Temst, C. V. Haesendonck, Y. Bruynseraede, A. Gilabert and I. K. Schuller: Phys. Rev. B **43** (1991) 8676.
6) W. E. Lawrence and S. Doniach: *Proc. 12th Int. Conf. Low Temperature Physics 1970*, ed. E. Kanda (Academic Press, Tokyo, 1971) p. 361.
7) R. A. Klemm, A. Luther and M. R. Beasley: Phys. Rev. B **12** (1975) 877.
8) G. Deutscher and O. Entin-Wohlman: Phys. Rev. B **17** (1978) 1249.
9) S. Takahashi and M. Tachiki: Phys. Rev. B **33** (1986) 4620.
10) S. Takahashi and M. Tachiki: Phys. Rev. B **34** (1986) 3162.
11) M. Tachiki and S. Takahashi: Physica B **169** (1991) 121.
12) H. Nakajima, Y. Obi, U. Fukumoto and H. Fujimori: J. Phys. Soc. Jpn. **56** (1987) 295.
13) M. Ikebe, Y. Obi, Y. Kamiguchi, Y. Fukumoto, H. Nakajima, Y. Muto and H. Fujimori: Jpn. J. Appl. Phys. **26** (1987) 1447.
14) Y. Obi, M. Ikebe, Y. Fukumoto, Y. Muto and H. Fujimori: *Superconducting Materials*, eds. S. Nakajima and H. Fukuyama (Publication Office, Jpn. J. Appl. Phys., Tokyo, 1988) JJAP Series 1, p. 129.
15) Y. Kamiguchi, M. Ikebe, Y. Obi and H. Fujimori: Jpn. J. Appl. Phys. **30** (1991) 945.
16) Y. Obi, M. Ikebe and H. Fujimori: Jpn. J. Appl. Phys. **31** (1992) 1334.
17) M. Ikebe, Y. Obi, H. Fujishiro and H. Fujimori: Jpn. J. Appl. Phys. **32** (1993) 117.
18) K. Kanoda, H. Mazaki, N. Hosoito and T. Shinjo: Phys. Rev. B **35** (1987) 6736.